

Ground state properties and dynamics of the bilayer $t - J$ model

R. Eder

*Department of Applied and Solid State Physics, University of Groningen,
9747AG Groningen, The Netherlands*

Y. Ohta and S. Maekawa

Department of Applied Physics, Nagoya University, Nagoya 464-01, Japan

We present an exact diagonalization study of bilayer clusters of $t - J$ model. Our results indicate a crossover between two markedly different regimes which occurs when the ratio J_{\perp}/J between inter-layer and intra-layer exchange constants increases: for small J_{\perp}/J the data suggest the development of 3D antiferromagnetic correlations without appreciable degradation of the intra-layer spin order and the $d_{x^2-y^2}$ hole pairs within the planes persist. For larger values of J_{\perp}/J local singlets along the inter-layer bonds dominate, leading to an almost complete suppression of the intra-layer spin correlation and the breaking of the intra-layer hole pairs. The ground state with two holes in this regime has s -like symmetry. The data suggest that the crossover may occur for values of J_{\perp}/J as small as 0.2. We present data for static spin correlation function, magnetic structure factor and spin gap. We calculate the momentum distribution and electronic spectral function of the "local singlet state" realized for large J_{\perp}/J , and show that it deviates markedly from that of a single layer, making it an implausible candidate for modelling high-temperature superconductors.

74.20.-Z, 75.10.Jm, 75.50.Ee

I. INTRODUCTION

In connection with the so-called spin-gap phenomenon [1] observed in high-temperature superconductors the properties of coupled layers of 2D $t - J$ model have recently attracted considerable attention [2–5]. In this work we present results obtained by exact diagonalization of small clusters, which may provide a rough guideline for this problem. Our data were obtained by diagonalization of clusters of size 2×8 and 2×10 , essentially the limit that can be reached by the exact diagonalization technique. Clearly these are still very small systems, and subtle low-energy effects certainly will escape our study. However, one may expect that even small clusters can mimic the short range correlation functions (which solely determine the total energy) roughly correct, and when interpreted with care our calculations thus may provide a crude phase diagram of the bilayer. Our key result is that already for fairly moderate values of the inter-layer exchange a qualitatively new type of ground state is realized, which deviates significantly from that of a single layer.

The model under consideration reads

$$H = - \sum_{\langle i,j \rangle, \sigma} t_{i,j} (\hat{c}_{i,\sigma}^{\dagger} \hat{c}_{j,\sigma} + H.c.) + \sum_{\langle i,j \rangle} J_{i,j} [\mathbf{S}_i \cdot \mathbf{S}_j - \frac{n_i n_j}{4}].$$

Here the \mathbf{S}_i are the electronic spin operators, $\hat{c}_{i,\sigma}^{\dagger} = c_{i,\sigma}^{\dagger} (1 - n_{i,-\sigma})$ and the sum over $\langle i, j \rangle$ stands for a

summation over all pairs of nearest neighbors. Our system consists of two planes, labelled A and B for later reference, the z -axis of the coordinate system is taken to be perpendicular to the planes. We distinguish between the hopping integral and exchange constant between nearest neighbors in the same plane, which we denote by t and J , and between nearest neighbors in different planes, which we denote by t_{\perp} and J_{\perp} . There is presently an unclear situation as to the correct choice of parameter values, experimental estimates for the ratio J_{\perp}/J vary from 0.085 [6], over 0.3 [7], up to 0.55 [8]. As for the inter-layer hopping integral t_{\perp} , the situation is even more unclear. Let us note that inter-layer hopping integrals derived from band structure calculations for cuprate superconductors are meaningless on the level of the $t - J$ model, because the "hole" in the $t - J$ model stands for an extended object, the Zhang-Rice singlet, which has very different hybridization matrix elements with orbitals outside the plane than a "bare" electron [9]. We will therefore consider different ratios of the various parameters and study their impact on e.g. the nature of the ground state.

II. UNDOPED BILAYER

To begin with, we briefly discuss the spin correlations of an undoped bilayer. Figure 1 shows the nearest-neighbor static spin correlation function in plane and

out-of plane as well as the spin structure factor for momentum transfer $(\pi, \pi, 0)$ and (π, π, π) . As J_{\perp}/J increases, there is initially a fairly symmetric splitting between $S(\pi, \pi, 0)$ and $S(\pi, \pi, \pi)$, their average $\bar{S}(\pi, \pi) = \frac{1}{2}(S(\pi, \pi, 0) + S(\pi, \pi, \pi))$ remaining almost constant. The latter quantity measures the antiferromagnetic correlations within a single plane. In this range of J_{\perp}/J , there is virtually no degradation of the antiferromagnetic order within the planes. The maximum of $S(\pi, \pi, \pi)$ is reached rather precisely for $J_{\perp}/J = 1$, and for this value the nearest neighbor spin correlation function within and between the planes are equal. Quite obviously, for this parameter value the bilayer is closest to a 3D Heisenberg antiferromagnet. When J_{\perp}/J is increased further, $\bar{S}(\pi, \pi)$ decreases and so does the intra-layer nearest neighbor spin correlation function. The spin correlations within the plane now decrease and local singlets along the inter-layer bonds start to dominate. However, the intra-plane correlations still are relatively "stiff", so that large values of J_{\perp}/J are required to bring them close to zero.

III. DOPED CASE

We next consider the doped bilayer, more precisely the ground states with two holes of the 2×8 and 2×10 bilayer. These show the same overall trends as the undoped bilayer, however within a much smaller range of J_{\perp}/J . Figure 2 shows the nearest neighbor spin correlation functions as functions of J_{\perp}/J and demonstrates that the crossover to a state with almost vanishing in-plane spin correlations and dominant z -axis spin correlations is much more abrupt than for the undoped system. Hole doping obviously makes it easier for the inter-plane terms to dominate over the in-plane exchange. The strong difference as compared to the undoped case moreover shows that results for undoped bilayer systems may have limited significance for the doped bilayer.

The second major difference as compared to the undoped bilayer is, that the crossover from the small to large J_{\perp}/J regime is now accompanied by a ground state level crossing. For small values of J_{\perp}/J the 2 hole ground state of the 2×10 bilayer belongs to the B_1 (or $d_{x^2-y^2}$) representation of the C_{4v} point group, reflecting the well-known fact [10] that two holes in the $t - J$ model always form a bound state with this symmetry. In this state, the two holes can be found in the same plane with high probability i.e. the in-plane bound state obviously persists to some degree. This changes completely when J_{\perp}/J is increased beyond a certain critical value: the ground state now has the A_1 (or s) symmetry and the two holes are in different planes almost with probability 1. A rough "phase diagram" of the 2×10 bilayer is given in Figure 3, Table I shows the hole density correlation function $g(\mathbf{R}) = \sum_i \langle (1 - n_i)(1 - n_{i+\bar{R}}) \rangle$ for both B_1 and A_1 state near the crossover. An analogous level crossing also can be found in the 2×8 cluster, for comparable val-

ues of J_{\perp}/J , so that it does not seem to originate from some spurious effect due to the special geometry of one of these two clusters. Strong inter-layer spin correlations thus are incompatible with d -wave pairing of holes within the planes, and change the symmetry properties of the ground state. It is interesting to note that the incompatibility of d -wave pairing within the planes and strong interlayer spin correlations has also been found by Liechtenstein *et al.* [11] within a weak coupling framework, as well as by Normand *et al.* [5] within slave-boson mean field theory. This seems to be a very general property of bilayer systems.

At this point, the possibility of fairly strong finite-size effects on the critical value of J_{\perp}/J becomes obvious: since the transition to the state with pronounced z -axis spin correlations implies the breaking of the in-plane pair, it follows that an overestimation of the in-plane hole binding energy will lead to an artificial stabilization of the "conventional" B_1 ground state. To see this, we first define the binding energy as $\Delta_B = (E_0^{(2h)} - E_0^{(0h)}) - 2 \cdot (E_0^{(1h)} - E_0^{(0h)}) = (E_0^{(2h)} + E_0^{(0h)}) - 2 \cdot E_0^{(1h)}$ where $E_0^{(\nu h)}$ denotes the ground state energy with ν holes. In small clusters of $t - J$ model this quantity is negative [10], so that in the limit $J_{\perp}, t_{\perp} \rightarrow 0$ the 2 hole ground state of the bilayer will approach a product of an undoped layer and a layer with two bound holes. The binding energy Δ_B then represents a kind of charge transfer energy, i.e. it gives the cost in energy upon transferring one of the two holes to the other layer. Hole binding within the planes thus opposes the formation of the A_1 state, and since it is known that finite-size calculations for the 2D $t - J$ model tend to substantially overestimate Δ_B [12], this may have an impact on the crossover between the two different ground states. In order to further investigate this issue, we add to the Hamiltonian a repulsive interaction between holes in the same plane:

$$H_V = V \left(\sum_{i,j \in A} n_i n_j + \sum_{i,j \in B} n_i n_j \right). \quad (1)$$

Such a term does not affect the intra-plane dynamics; it only reduces the loss of energy which occurs when a hole is transferred between the two layers. In particular, if we adjust $V = \Delta_B$ this term precisely cancels the effects of the in-plane binding energy which may contain large finite-size effects. Figure 4 then shows (for the value $J/t = 0.4$) the change of the crossover value of $(J_{\perp}/J)_{crit}$ when the in-plane repulsion is increased. There is an obvious linear dependence and for completely "balanced" intra-layer binding energy (i.e. for vanishing hole transfer energy) we find $(J_{\perp}/J)_{crit} = 0.17$. For $J/t = 0.2$ the same procedure gives $(J_{\perp}/J)_{crit} = 0.15$ (for completely balanced binding energy), so that in the parameter region of possible relevance for cuprate superconductors the crossover to the unpaired state may occur for fairly small values of J_{\perp}/J .

For completeness we have to address possible ground state degeneracies. For the single 10-site cluster with

periodic boundary conditions there exists a special permutation of the sites which leaves all nearest neighbor relations invariant; this is analogous to the well-known 2^4 hypercube symmetry of the 4×4 cluster with periodic boundary conditions [10]. This artificial symmetry operation therefore commutes with any Hamiltonian involving only nearest neighbor terms and introduces artificial degeneracies. Clearly, for the 2×10 bilayer there exists an analogous permutation of z -axis bonds, leading to artificial degeneracies as well. We have always neglected the degenerate ground states with finite momentum, because we believe that the ground state with vanishing momentum is the most natural representative of the infinite system. In the single layer case, this is confirmed by the fact that the $\vec{k} = 0$ ground states of different clusters all have very analogous properties, whereas the degenerate finite momentum ground states disappear for larger clusters. It is moreover straightforward to see, that these degenerate states cannot add much new information: for example the average nearest neighbor spin correlation functions can be expressed as derivatives of the total energy with respect to the exchange constants J and J_\perp , the probability to find the two holes in different planes is related to the derivative with respect to the parameter V in (1), so that these quantities must be rigorously the same for all symmetry-degenerate ground states.

We now turn to the spin correlations, shown in Figures 5 and 6. The B_1 state shows the same symmetric splitting of $S(\pi, \pi, 0)$ and $S(\pi, \pi, \pi)$ which was seen already in the undoped spin-bilayer; the inter-plane spin correlations increase only moderately. Quite obviously, in this state the development of inter-layer spin correlations is accomplished by the "lock in" of the directions of the local staggered magnetization M_S in the two planes, with essentially unchanged intra-plane correlations. By contrast, the A_1 state shows dominant inter-plane correlations and, as shown in Figure 2, already for values of $J_\perp/J \sim 1$ it rapidly approaches the limit of a product state of z -axis singlets.

In order to further clarify the mechanism by which inter-layer spin correlations are built up, we now study the probability distribution of the staggered magnetization in the ground state. More precisely, we denote by $\mathcal{M}_{\mu,\nu}$ the set of basis states which have staggered magnetization μ in the A-plane and staggered magnetization ν in the B-plane. Then, we can define the operator

$$\mathcal{P}_{\mu,\nu} = \sum_{\alpha \in \mathcal{M}_{\mu,\nu}} |\Phi_\alpha\rangle \langle \Phi_\alpha|,$$

and its ground state expectation value $S(\mu, \nu) = \langle \mathcal{P}_{\mu,\nu} \rangle$. It may be interpreted as the total weight of states with single-layer staggered magnetizations μ and ν . Figure 7 shows this quantity for two values of J_\perp/J . For vanishing inter-layer coupling the ground state is simply the product of two single-layer ground states, and if one chooses fixed z -component of the momentum, $S(\mu, \nu)$ must be completely symmetric, i.e. $S(\mu, \nu) = S(\mu, -\nu) =$

$S(-\mu, \nu) = S(-\mu, -\nu)$. The data then show, that for increasing J_\perp/J there is first a slight shift of weight from the $(+, +)$ and $(-, -)$ quadrants to the $(+, -)$ and $(-, +)$ quadrants: the staggered magnetization of the two layers "locks in". However, states with large staggered magnetization still do have appreciable weight, and the correlation between the values of M_S in the two planes is not yet strong. This changes completely when we increase J_\perp/J beyond the crossover to the A_1 ground state: $S(\mu, \nu)$ is now concentrated near the line $\mu = -\nu$, and along this line it drops sharply towards large values of M_S . The values of M_S in the two layers are now strongly correlated: when there is e.g. a fluctuation towards a large positive value of M_S in the A-plane, it must be accompanied by a fluctuation to a large negative value in the B-plane. These results are precisely what one would expect if the spins were distributed randomly within the planes, but under the constraint that nearest neighbor spins in z -direction always be antiparallel. Analysis of the probability distribution $S_{\mu,\nu}$ thus confirms the scenario inferred from the spin correlation function: there is a regime of small J_\perp/J , where the system responds to the inter-layer coupling by a weak "lock-in" of the staggered magnetization in the two planes, while no appreciable change of the intra-layer correlations takes place. For large J_\perp/J , on the other hand, we have the clear signatures of the z -axis singlet state.

We next consider the "spin gap", defined as

$$\Delta_{spin} = E_{0,\Gamma_0}(\pi, \pi, \pi) - E_0$$

Here E_0 denotes the energy of the ground state (which has momentum 0) and $E_{\Gamma_0}(\pi, \pi, \pi)$ denotes the lowest energy in the subspace of states with momentum (π, π, π) and the same point group symmetry Γ_0 as the ground state. Inspection shows that the $\vec{k} = 0$ ground state is always a singlet, the (π, π, π) state always a triplet, so that Δ_{spin} indeed represents the gap which would be observed in the dynamical spin correlation function with momentum transfer (π, π, π) . We note that Δ_{spin} is prone to massive finite-size effects, as can be seen e.g. from the fact that even an undoped 2D cluster has a "spin gap" of $\approx 0.4J$ [13]. The values of Δ_{spin} determined from the small clusters thus may at best indicate a rough qualitative trend, but clearly have no quantitative significance. Then, Figure 8a shows the spin gap over a wide range of J_\perp/J . It is remarkable that the gap initially *decreases* with increasing J_\perp and in fact shrinks appreciably at the level crossing to the strong z -axis correlation (A_1) state. It is only for values of $J_\perp/J > 1$ that the spin gap becomes large and grows linearly with J_\perp , reflecting the saturation of the z -axis spin correlation function (see Figure 2). For an undoped system and in the limit $J_\perp/J \rightarrow \infty$ it is easy to see that a single z -axis *triplet* bond can propagate in a "background" of z -axis singlets with a nearest neighbor hopping element of $J/2$, so that the spin gap should be $J_\perp - z \cdot (J/2)$, with z the number of nearest neighbor z -axis bonds. The resulting asymptotic expressions $\Delta_{spin} = J_\perp - J$ for the ladder ($z = 2$) and

$\Delta_{spin} = J_{\perp} - 2J$ for the bilayer ($z = 4$) indeed provide excellent estimates for the undoped systems (compare Figure 2 in Ref. [2]); for the doped system, however, the numerical result rather suggests the asymptotic expression $\Delta_{spin} = J_{\perp} - (J/2)$, which would imply a reduction of the effective hopping element for the triplet-bond by a factor of 4. This indicates, that the propagation of the z -axis triplet is inhibited by the presence of mobile holes, so that there must be a strong interplay between the local singlets/triplets and the holes.

Figure 8b shows the spin gap for other parameter values in the range $J_{\perp}/J < 1$ and demonstrate that increasing values of J_{\perp}/J initially tend to reduce Δ_{spin} , as would be expected from an enhancement of antiferromagnetic correlations. It is interesting to note that the crossover $B_1 \rightarrow A_1$ never leads to an increase of Δ_{spin} . While the significance of these data should not be overestimated, we may state that in the small clusters there is no indication of any widening of the spin gap due to interlayer coupling, at least not for "reasonable" values of J_{\perp}/J .

IV. LOCAL SINGLET STATE

We now proceed to a study of the "z-axis singlet state", which is realized for larger J_{\perp}/J . As has been shown above, this state may appear already for quite moderate values of $J_{\perp}/J \approx 0.2$, which have in fact been postulated to be realized in actual high-temperature superconductors. In fact, this state may be considered a qualitatively new feature of the bilayer system, as compared to the single-layer ground states studied extensively before. We first consider the limiting case of vanishing in-plane parameters J and t [2]. Depending on the relative magnitude of t_{\perp} and J_{\perp} , the ground state of the $2 \times N$ bilayer with an even number of holes n_h can take two quite different forms (see Figure 9): it is either the product of $N - n_h/2$ z -axis singlets and $n_h/2$ empty z -axis bonds with energy $(N - n_h/2) \cdot J_{\perp}$; or it is a product of $N - n_h$ z -axis singlets and n_h singly occupied z -axis bonds with energy $(N - n_h) \cdot J_{\perp} - n_h \cdot t_{\perp}$. The degeneracy of this ground state is lifted by the intra-plane terms of the Hamiltonian. We assume that the most important intra-plane term in the Hamiltonian is the hopping integral t . Then, a singly occupied bond can propagate to a nearest neighbor in a single-step process with the effective hopping integral $t/2$, whereas an empty bond propagates to a nearest neighbor via a two step process where the intermediate state has a broken z -axis singlet; in the regime of large J_{\perp}/t perturbation theory would give an effective hopping integral $\sim t^2/J_{\perp}$. We thus have the interesting situation that, depending on the relative strength of parameters, two very different "fixed points" may be appropriate to describe the bilayer system: if the arrangement of holes in empty bonds is preferred, the system should correspond to a gas of $n_h/2$ hard core bosons, propagating via nearest neighbor hopping of strength $\sim t^2/J_{\perp}$. On the other hand, if

the arrangement of holes along singly occupied bonds is preferred, the bilayer should correspond to a system of n_h spin-1/2 fermions, propagating via nearest neighbor hopping of strength $t/2$. In both cases, however, there is a positive nearest neighbor hopping matrix element for either hole-like "Fermion" or "Boson", so that the holes may be expected to accumulate at the in-plane momentum (π, π) .

The calculated values of the electron momentum distribution function $n(\vec{k}) = \langle \hat{c}_{\vec{k},\sigma}^{\dagger} \hat{c}_{\vec{k},\sigma} \rangle$, given in Tables II and III, then indeed show an enhanced hole-occupancy of (π, π) in the A_1 state even for moderate values of J_{\perp} and t_{\perp} : this is very pronounced in the 2×8 system, but also in the 2×10 bilayer one can realize an enhanced depression at (π, π) and a tendency towards the "flattening" of $n(\vec{k})$ in the remainder of the Brillouin zone. This indicates that the momentum distribution with "hole pockets" at (π, π) , which would be expected in the limit of large inter-layer coupling indeed seems to persist in the A_1 state also for moderate values of the inter-layer coupling. This picture is confirmed by the single particle spectral function $A(\mathbf{k}, \omega)$, shown in Figure 10. Due to restrictions in computer memory, we have evaluated this quantity only for the 2×8 bilayer. The topmost peaks in the photoemission spectra are located at $(\pi/2, \pi/2)$ and $(\pi, 0)$ (due to the special symmetry of the $2D$ 8-site cluster these momenta are in fact identical for the A_1 state), but there is no appreciable low energy weight in the inverse photoemission spectrum at either of these momenta: quite obviously these k -points are "occupied". This is in clear contrast to the spectral function for the B_1 state [14] which showed a rather obvious Fermi level crossing at $(\pi, 0)$. Another notable feature is the strong contrast between the relatively sharp peaks in the bonding channel (i.e. $k_z = 0$) and the more diffuse spectra in the antibonding one, which have markedly enhanced incoherent continua. This indicates that electrons in the bonding channel are the "more well-defined" excitations of the system, as one would expect it for a product state of doubly and singly occupied bonds. The strong difference between the $k_z = 0$ and $k_z = \pi$ spectra is again in contrast to their almost identical shape in the B_1 ground state [14]. The available data thus rather consistently suggest that even for moderate values of J_{\perp} and t_{\perp} the "z-axis singlet state" bears a strong resemblance to the $J_{\perp}, t_{\perp} \rightarrow \infty$ limit, which in particular implies the accumulation of holes at (π, π) .

V. SUMMARY AND DISCUSSION

In summary, we have studied the effects of interlayer exchange in a bilayer $t - J$ model. The data rather consistently suggest a crossover between two very different regimes: for small and moderate values of the inter-plane exchange coupling there is no qualitative change of the

spin correlations, the in-plane hole pairing with $d_{x^2-y^2}$ symmetry persists and the inter-plane exchange induces 3D antiferromagnetic correlations. For increasing values of J_{\perp}/J there is a crossover to a state with dominant inter-layer spin correlations, where the intra-layer hole pairing is completely suppressed. We note that this feature may well persist in the infinite system if the pairing state remains short ranged; in this case, it would be the short range correlations which dominate the physics, and these may be expected to be described properly even in the small clusters. The data finally do not show any indication of a widening of the spin gap at the crossover. The result that strong inter-layer coupling suppresses the in-plane $d_{x^2-y^2}$ pairing clearly would be hard to reconcile with the ever growing experimental evidence for d -type symmetry of the superconducting order parameter in the cuprate superconductors [15] and the experimental fact that T_c seems to increase with the number of closely coupled layers in these compounds. In addition, our data indicate that the "z-axis singlet state" realized for large J_{\perp}/J has fairly unusual properties such as a tendency towards "hole pockets" at the in-plane momentum (π, π) , so that it does not seem to be a very promising candidate for modelling real high-temperature superconductors. Moreover, the relatively strong difference between the z-axis singlet state and the "conventional" single layer ground state would make it hard to understand why many properties of single and double layer cuprates are relatively similar.

Clearly, the simplest way to resolve these problems is to assume that the values of J_{\perp}/J in the actual materials are too small to ever induce the z-axis singlet state. Unfortunately strong finite size effects do not allow us to give a very accurate estimate of the critical value where the crossover occurs. Then, a possible enhancement of antiferromagnetic spin correlations due to the onset of 3D correlations in the more conventional ground states realized for lower J_{\perp}/J may be more easy to reconcile with experiment: it seems plausible that pairing theories which rely on antiferromagnetism, such as the antiferromagnetic spin fluctuation theory [16] or the antiferromagnetic van-Hove scenario [17] would profit from the onset of 3D correlations, so that the exchange coupling of several CuO_2 planes could be favourable for achieving higher T_c 's.

We thank Dr. W. Koshibae for help with preparing the manuscript. Financial support of R. E. at Nagoya by the Japan Society for the Promotion of Science is most gratefully acknowledged. Support of R. E. at Groningen by the European Community is most gratefully acknowledged, too.

TABLE I. Comparison of the hole density correlation function $g(\vec{R})$ in the lowest state with B_1 symmetry and the lowest state with A_1 symmetry of the 2×10 bilayer $t - J$ model. Parameter values are $t = 1$, $J = 0.4$, $t_{\perp} = 0.5$, $J_{\perp}/J = 0.8$. The value of J_{\perp}/J is chosen slightly above the crossover $B_1 \rightarrow A_1$, so that the A_1 state is the ground state, the B_1 state being 0.0289 above the ground state.

	$R_{in-plane}$			
B_1	(0, 0)	(1, 0)	(1, 1)	(2, 1)
$R_z = 0$	0.000	0.0791	0.0943	0.0898
$R_z = 1$	0.0189	0.0243	0.0213	0.0151
A_1	(0, 0)	(1, 0)	(1, 1)	(2, 0)
$R_z = 0$	0.000	0.0115	0.0095	0.0119
$R_z = 1$	0.2217	0.1038	0.0573	0.0380

TABLE II. Comparison of the momentum distribution function $n(\vec{k})$ for the lowest state with A_1 symmetry and the lowest state with B_1 symmetry of the 2×10 bilayer $t - J$ model. Parameter values are like in Table 1.

	$k_{in-plane}$			
A_1	(0, 0)	$(\frac{3\pi}{5}, \frac{\pi}{5})$	$(\frac{2\pi}{5}, \frac{4\pi}{5})$	(π, π)
$k_z = 0$	0.5357	0.5321	0.4367	0.2757
$k_z = \pi$	0.5214	0.4730	0.3966	0.3132
B_1	(0, 0)	$(\frac{3\pi}{5}, \frac{\pi}{5})$	$(\frac{2\pi}{5}, \frac{4\pi}{5})$	(π, π)
$k_z = 0$	0.5399	0.5278	0.4374	0.3424
$k_z = \pi$	0.5416	0.4815	0.3668	0.3223

TABLE III. Comparison of the momentum distribution function $n(\vec{k})$ for the lowest state with A_1 symmetry and the lowest state with B_1 symmetry of the 2×8 bilayer $t - J$ model. The value of $J_{\perp}/J = 0.6$ is chosen slightly above the crossover $B_1 \rightarrow A_1$, so that the A_1 state is the ground state, the B_1 state being 0.0154 above the ground state. The other parameter values are $t = 1$, $J = 0.4$, $t_{\perp} = 0.5$.

	$k_{in-plane}$			
A_1	(0, 0)	$(\frac{3\pi}{5}, \frac{\pi}{5})$	$(\frac{2\pi}{5}, \frac{4\pi}{5})$	(π, π)
$k_z = 0$	0.5446	0.5014	0.5014	0.16574
$k_z = \pi$	0.5017	0.4213	0.4213	0.2518
B_1	(0, 0)	$(\frac{3\pi}{5}, \frac{\pi}{5})$	$(\frac{2\pi}{5}, \frac{4\pi}{5})$	(π, π)
$k_z = 0$	0.5469	0.5260	0.4410	0.2915
$k_z = \pi$	0.5444	0.4624	0.2525	0.2761

FIG. 1. (a) Static nearest neighbor spin correlation function $\langle \vec{S}_i \cdot \vec{S}_j \rangle$ for the ground state of the undoped 2×10 bilayer. (b) Static spin structure factors $S(\pi, \pi, 0)$ (diamonds) and $S(\pi, \pi, \pi)$ (crosses) and average $\bar{S}(\pi, \pi)$ (squares) for the same state.

FIG. 2. Static nearest neighbor spin correlation function $\langle \vec{S}_i \cdot \vec{S}_j \rangle$ for the ground state of the 2×10 bilayer with two holes. Parameter values are $t = 1$, $J = 0.2$, $t_{\perp} = 0.1$.

FIG. 3. "Phase diagram" for the 2×10 bilayer with two holes for two values of t_{\perp}/t . The figure indicates the regions of stability of the A_1 and B_1 ground state for different parameter values. The respective critical values of J_{\perp}/J have been obtained by interpolating ground state energies and are accurate only to $\sim \pm 0.05$.

FIG. 4. Critical value of $(J_{\perp}/J)_{crit}$ for the crossing $B_1 \rightarrow A_1$ as a function of the intra-plane repulsion parameter V .

FIG. 5. Nearest neighbor spin correlation function $\langle \vec{S}_i \cdot \vec{S}_j \rangle$ for the 2×10 bilayer with two holes. (b) Static spin structure factors $S(\pi, \pi, 0)$ (diamonds) and $S(\pi, \pi, \pi)$ (crosses) and average $\bar{S}(\pi, \pi)$ (squares) for the same system. Parameter values are $t = 1$, $J = 0.4$, $t_{\perp} = 0.5$.

FIG. 6. Same as Figure 4 for $J = 0.2$.

FIG. 7. Probability distribution $S_{\mu,\nu}$ for the ground state of the 2×8 bilayer with two holes and different J_{\perp}/J . The distribution has been averaged over the areas indicated in the figure. Parameter values are $J_{\perp}/J = 0.4$ (a) and $J_{\perp}/J = 1$ (b), the other parameters are $t = 1$, $J = 0.4$, $t_{\perp} = 0.5$ for both figures.

FIG. 8. (a) Spin gap Δ_{spin} as a function of J_{\perp}/J for $J = 0.2$, $t_{\perp} = 0.1$, 2×10 bilayer. (b) Δ_{spin} for different parameter values in the 2×10 bilayer, $t = 1$.

FIG. 9. Possible ground states of the bilayer model in the limit $t, J \rightarrow 0$: the holes are on "singly occupied bonds" (a) or on "empty bonds" (b).

FIG. 10. Single particle spectral function $A(\mathbf{k}, \omega)$ for the 2×8 bilayer. The vertical line marks the Fermi energy, the frequency range $\omega > E_F$ ($\omega < E_F$) corresponds to electron creation (annihilation). The full (dashed) line refers to the bonding (antibonding) channel. Parameter values are like in Table III.

-
- [1] H. Yasuoka *et al.*, in *Strong Correlations and Superconductivity*, Eds. H. Fukuyama, S. Maekawa, and A. P. Malozemoff, Springer Series in Solid State Sciences **89**, 254, (1989).
 - [2] E. Dagotto, J. Riera, and D. Scalapino, Phys. Rev. B **45**, 5744 (1992).
 - [3] A. J. Millis and H. Monien, Phys. Rev. Lett. **70**, 2810 (1993); Phys. Rev. B **50**, 16606 (1994).
 - [4] M. Ubbens and P.A. Lee, Phys. Rev. B **50**, 438 (1994); K. Kuboki and P.A. Lee, preprint.
 - [5] B. Normand, H. Kohno, and H. Fukuyama, preprint.
 - [6] J. Rossat-Mignot, *et al.*, in *Dynamics of Magnetic Fluctuations in High-Temperature Superconductors*, Eds. G. Reiter, P. Horsch and G. C. Psaltakis, NATO-ASI Series B, Vol. 246, 35 (1991).
 - [7] R. Stern *et al.*, preprint.
 - [8] M. Grüninger *et al.*, SISSA preprint.
 - [9] For example it is straightforward to see that due to its nontrivial symmetry the Zhang-Rice singlet on a given plaquette has vanishing hybridization with both the Cu 4s orbital on the central Cu atom and with any p orbital of the apex oxygen. Z -axis propagation is only possible via orbitals in neighboring plaquettes.
 - [10] Y. Hasegawa, D. Poilblanc, Phys. Rev. B **40**, 9035 (1989).
 - [11] A. I. Liechtenstein, I. I. Mazin, and O. K. Andersen, Phys. Rev. Lett. **74**, 2303 (1995).
 - [12] M. Bonisegni and E. Manousakis, Phys. Rev. B **43**, 10353 (1992).
 - [13] More precisely, the values are $0.329J$ for 16 sites, $0.506J$ for 18 sites and $0.467J$ for 20 sites.
 - [14] R. Eder, Y. Ohta, and S. Maekawa, Phys. Rev. B **51**, 3265 (1995).
 - [15] D.A. Wollman *et al.*, Phys. Rev. Lett. **71**, 2134 (1993); J. R. Kirtley *et al.*, Nature **373**, 225 (1995).
 - [16] T. Moriya, Y. Takahashi, and K. Ueda, J. Phys. Soc. Jpn. **49**, 2905 (1990); P. Monthoux, A. Balatsky, and D. Pines, Phys. Rev. Lett. **67**, 3448 (1991).
 - [17] E. Dagotto *et al.* Phys. Rev. Lett. **74**, 310 (1995).

Figure 1

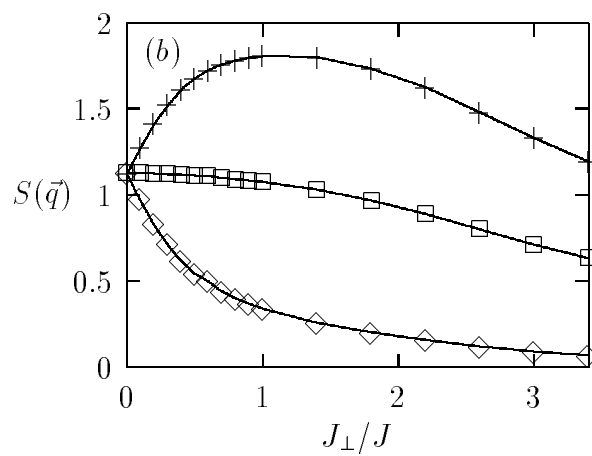
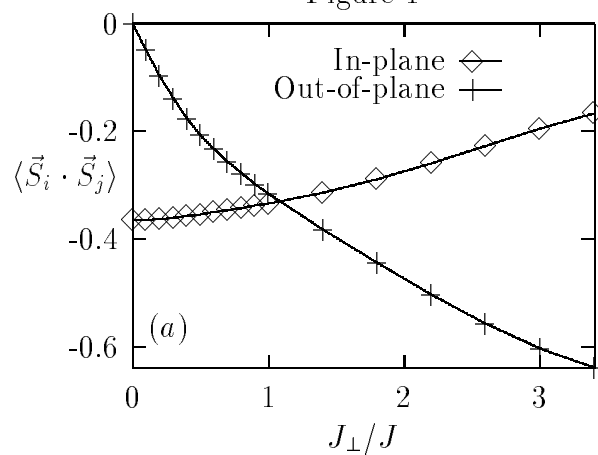


Figure 2

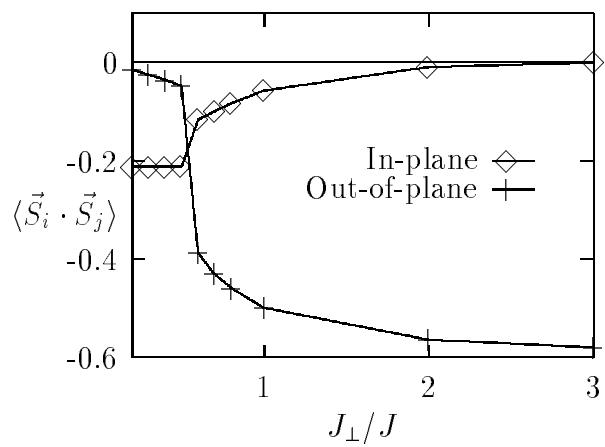


Figure 3

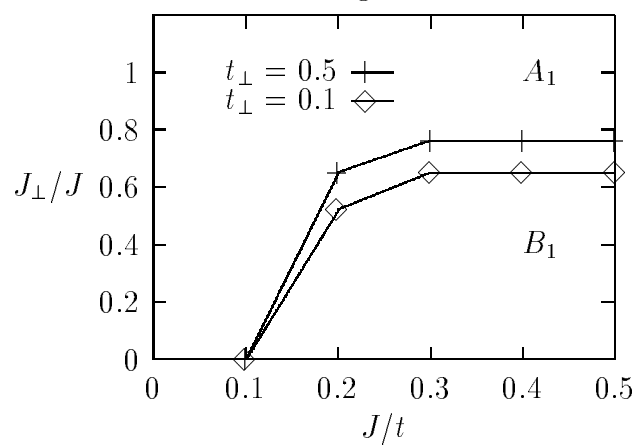


Figure 4

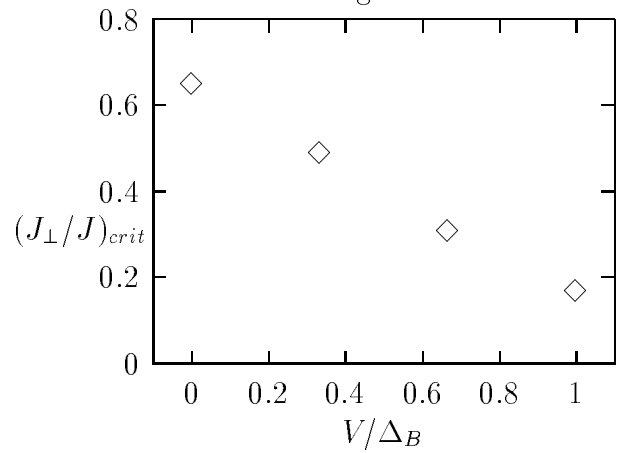


Figure 5

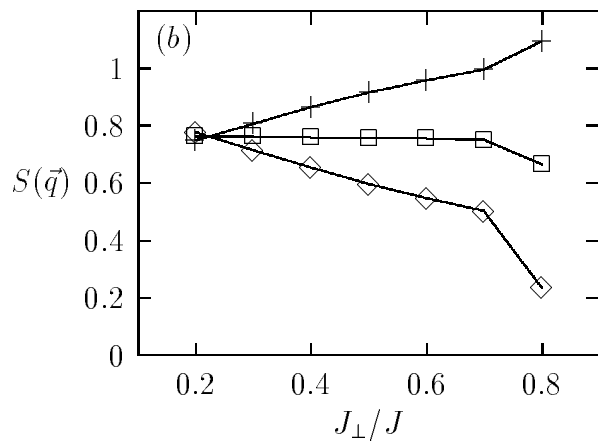
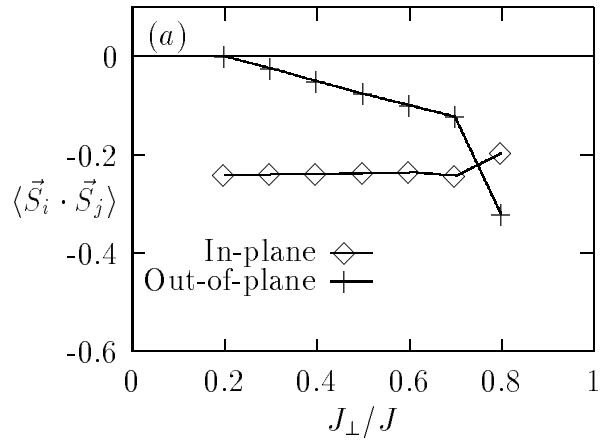


Figure 6

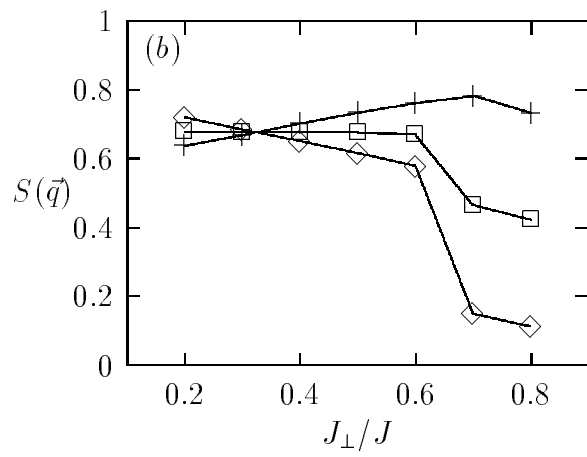
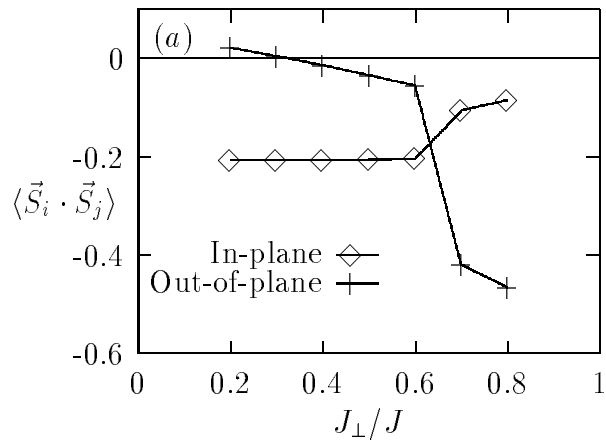
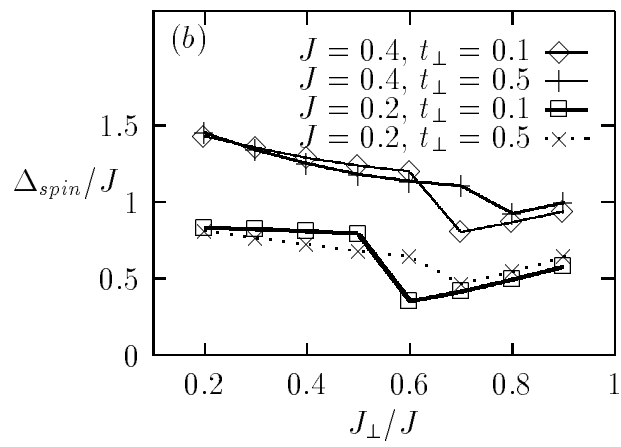
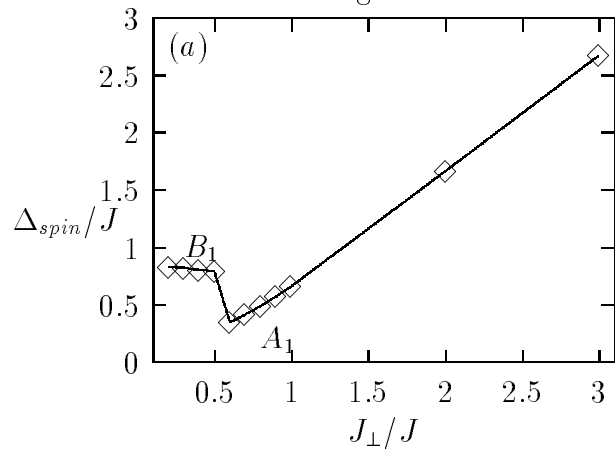


Figure 8



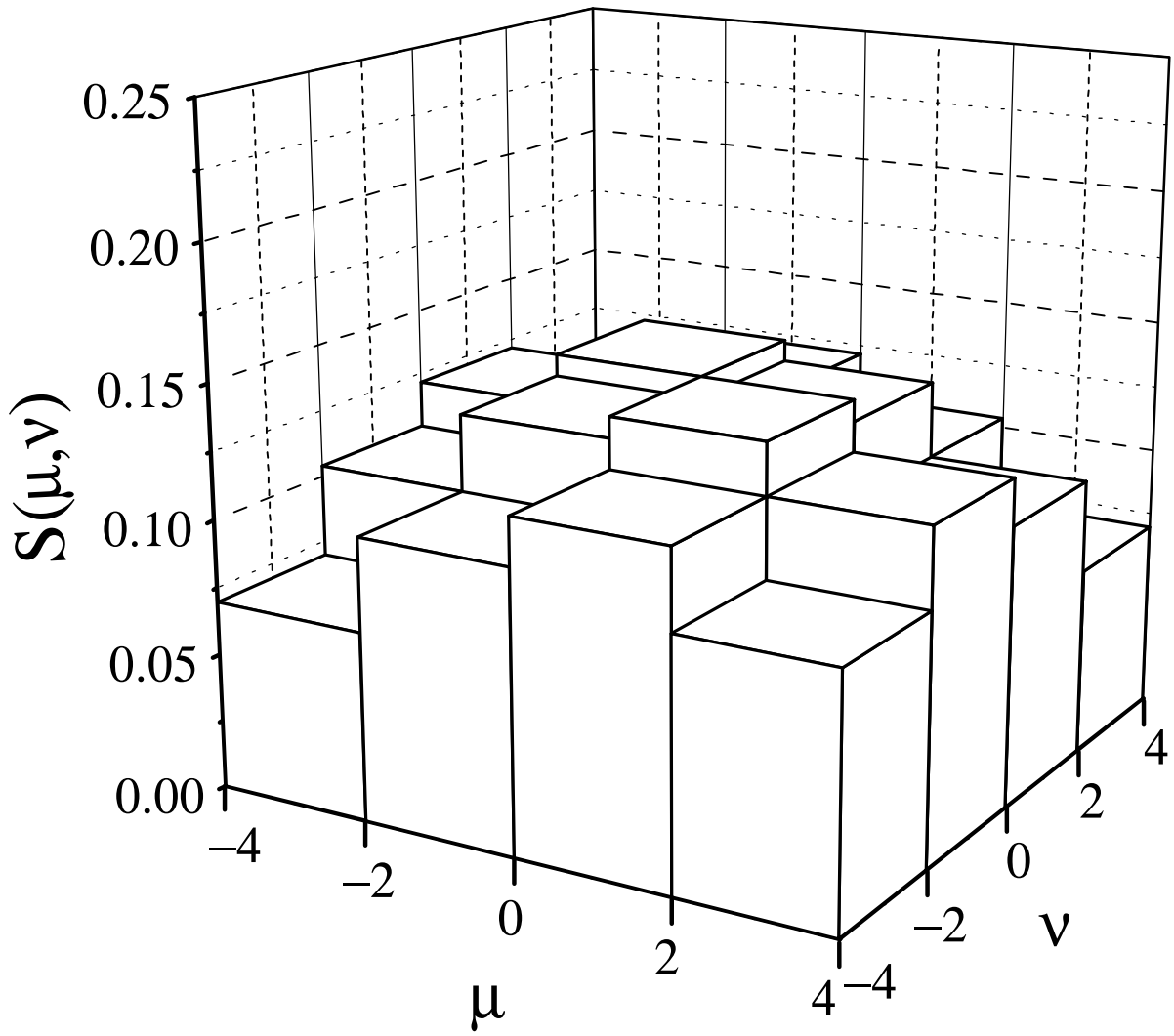


Fig. 7a

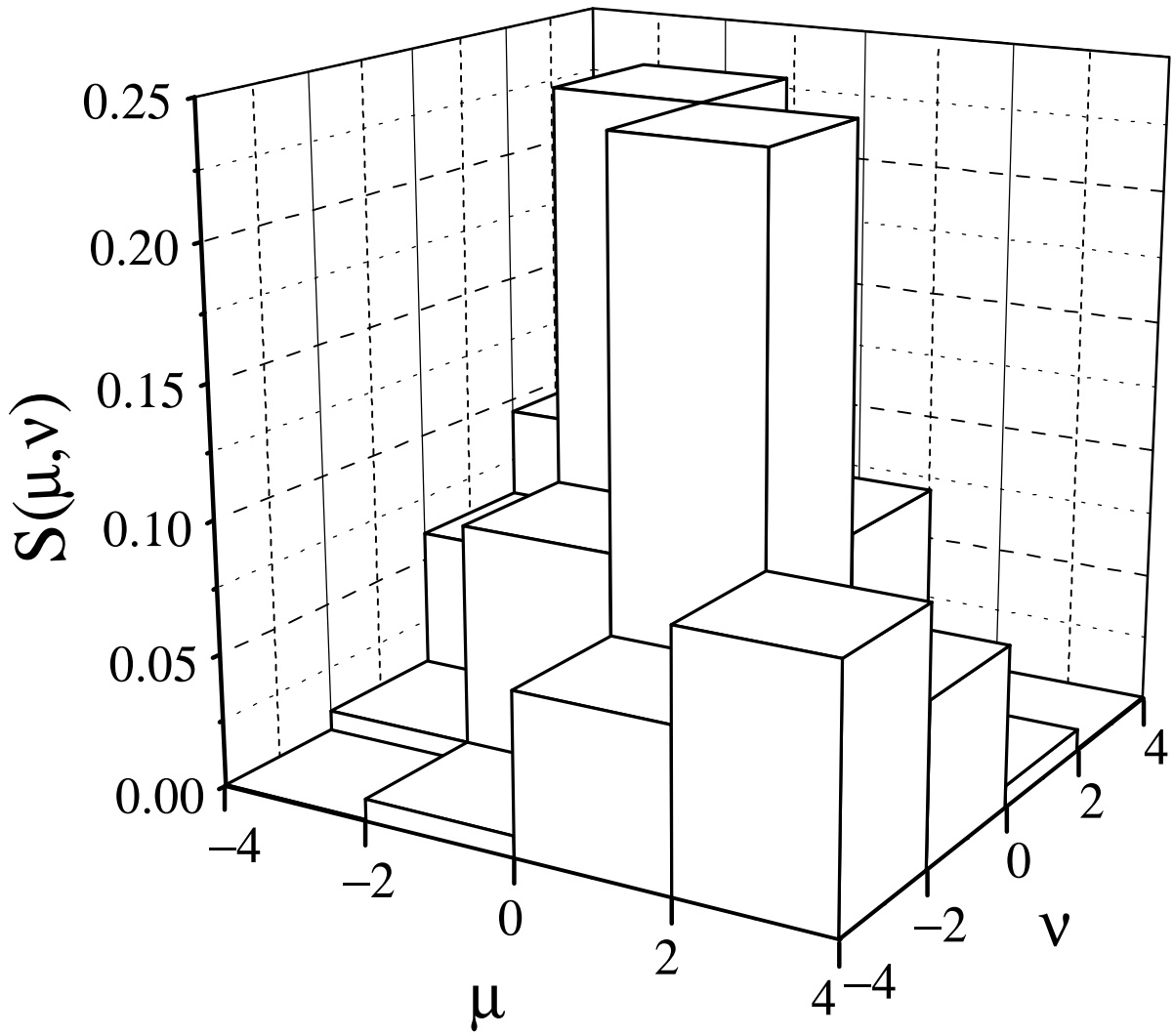


Fig. 7b

Figure 9

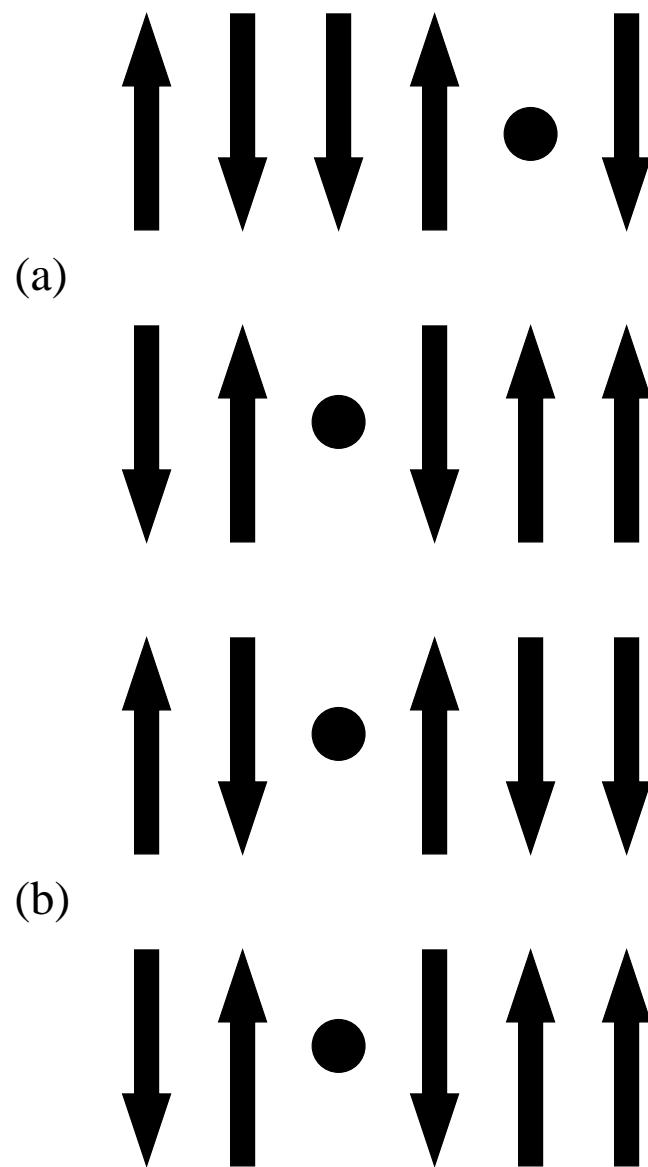


Figure 10

